eye observation. Naked eye observations indicated that the boundary shock was either in the cold or hot position and never stable between these two positions. In fact, with the electron beam sweeping at 7.5 Hz, no intermediate locations were detected at any time. The model rocket nozzle reservoir pressure, p_c, was increased from 258 torr to 323 torr and the jump was observed to occur at $T_c = 358°K$ instead of 340°K.

Experiments were continued using a smaller rocket nozzle with $A/A^* = 17.4$ and $r_e = 0.0825$ cm and a boundary shock jump was not detected for the reservoir conditions considered. Measured values of s/r_e are presented as a function of $(p_c/q_\infty)^{1/2}$ in Fig. 3. Apparently all values of s/r_e for the smaller nozzle correspond to the cold shock location. Unfortunately, due to limitations of chamber time, the effects of rocket nozzle dimensions, reservoir conditions, etc., on the boundary jump phenomenon could not be investigated further.

An approximate analytical result for the centerline plume boundary location for a nozzle plume exhausting counter to a supersonic freestream has been obtained in Ref. 1, using perfect gas, isentropic flow, and normal shock relations. The nozzle plume was assumed to be adequately described by the method of Ref. 2. The approximate result was obtained by assuming the freestream and plume gas static pressures between the normal boundary shocks on the nozzle center line were equal. The resulting analytical expression is

$$\tilde{s} = \frac{s}{r^*}\left(\frac{q_\infty}{p_c}\frac{1}{\gamma_\infty+1}\right)^{1/2} = \left[\frac{4\gamma_p B}{(\gamma_p+1)(\gamma_p-1)}\right]^{1/2} \quad (1)$$

where r^* is the rocket nozzle throat radius, γ_p is the ratio of specific heats of the plume gas, γ_∞ is the ratio of specific heats of the freestream gas, and B is a parameter which describes the density decay along the axis of the rocket nozzle plume. The parameter B is a function of γ_p and A/A^* and an approximate solution for B is given in Ref. 2. Comparisons between calculated and measured centerline plume boundary locations are presented in Fig. 3. The comparisons in Fig. 3 indicate the calculated boundary locations to be in better agreement with the cold shock positions than the hot shock positions. This is somewhat surprising because the boundary jump phenomenon has been attributed to condensation,[1] and, therefore, the calculated locations would presumably be more representative of the hot shock locations. Based on the comparisons in Fig. 3, two possible conclusions come to mind: 1) either the agreement with the cold shock data is fortuitous, i.e., the analysis is incorrect, or 2) condensation is not the primary cause of the boundary jump phenomenon.

Calculated values of $\tilde{s}$ as a function of A/A^* are presented in Fig. 4 for various γ_p. The assumption of constant γ_p is sometimes questionable for rocket exhaust plumes. However, γ_p is usually small for rockets and according to Fig. 4 the effect of γ_p on $\tilde{s}$ decreases with decreasing γ_p.

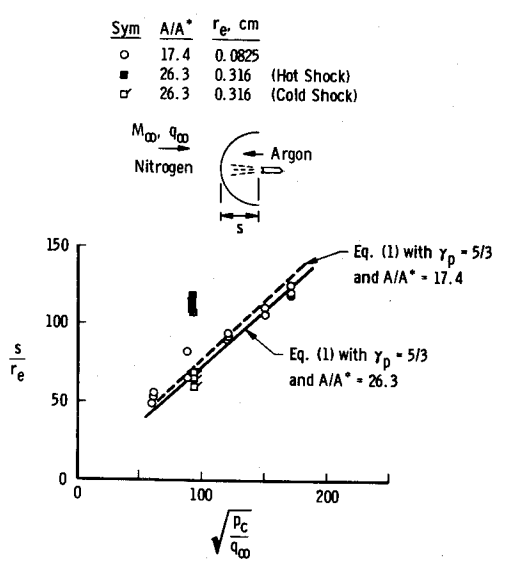

Fig. 3 Centerline plume boundary location as a function of $(p_c/q_\infty)^{1/2}$.

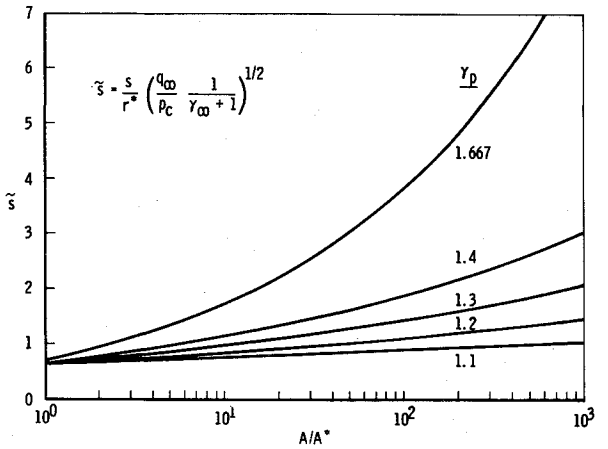

Fig. 4 Theoretical centerline plume boundary location for rocket nozzle exhausting counter to a supersonic freestream.

References

[1] Smithson, H. K., Price, L. L., and Whitfield, D. L., "Wind Tunnel Testing of Interactions of High Altitude Rocket Plumes with the Freestream," AEDC-TR-71-118, Sept. 1971, Arnold Engineering Development Center, Arnold Air Force Station, Tenn.

[2] Jarvinen, P. O., Hill, J. A. F., Draper, J. S., and Good, R. E., "High Altitude Rocket Plumes," Rept. MC 65-120-R3, June 1966, MITHRAS Inc., Cambridge, Mass.

Viscous Shock Layer Flow in the Windward Plane of Cones at Angle of Attack

ROGER R. EATON* AND PETER C. KAESTNER†
Sandia Laboratories, Albuquerque, N. Mex.

Nomenclature

M_∞ = freestream Mach number
p = pressure, N/m^2
Q = rate of heat transfer, joule/sec m^2
r = distance from body centerline to body surface, m
s = coordinate in crossflow direction, rad
u, v, w = velocity in x, y, and s directions, m/sec
x = coordinate measured along body from nosetip, m
y = coordinate perpendicular to body surface, m
y_{sh} = shock standoff distance, m
α = angle of attack
γ = ratio of specific heats
θ = slope along body surface

Presented as Paper 73-134 at the AIAA 11th Aerospace Sciences Meeting, Washington, D.C., January 10–12, 1973; submitted January 30, 1973, revision received April 19, 1973. The authors wish to acknowledge F. G. Blottner for his assistance on the problem. This work was supported by the U.S. Atomic Energy Commission.

Index category: Viscous Nonboundary-Layer Flows.

* Member Technical Staff. Member AIAA.
† Member Technical Staff.

μ = gas viscosity, Nsec/m^2
ρ = density, kg/m^3
χ = longitudinal body curvature

Introduction

A METHOD is developed for obtaining the viscous flow between the surface and shock in the windward plane of a sharp body at angle of attack. Shock layer solutions are obtained using a single set of equations which are developed from the steady-state Navier-Stokes equations for an ideal gas. Terms up to second order in the inverse square root of the Reynolds number are retained from both the viscous and inviscid points of view. The method developed by Davis[1] for bodies at zero angle of attack is extended to include the more general nonzero case. To solve this problem, the crossflow momentum equation is used and crossflow terms are retained in the flow equations. The details of this analysis are given in Ref. 2.

Analysis and Method of Solution

The energy and x-momentum equations are the same as those used in Ref. 1. An additional crossflow term is added to the continuity equation resulting in

$$\frac{\partial}{\partial x}[(r+y\cos\theta)\rho u]+\frac{\partial}{\partial y}[(r+y\cos\theta)(1+\chi y)\rho v]+\frac{\partial}{\partial s}[(1+\chi y)\rho w]=0 \qquad (1)$$

The normal momentum equation when simplified with the thin shock-layer approximation and zero longitudinal body curvature yields $\partial p/\partial y = 0$. The crossflow momentum equation which must be used has the form

$$\rho u\frac{\partial w}{\partial x}+\rho v\frac{\partial w}{\partial y}+\frac{\rho w}{r}\frac{\partial w}{\partial s}+\frac{\rho uw}{r}\frac{\partial r}{\partial x}=-\frac{1}{r}\frac{\partial p}{\partial s}+\frac{\partial}{\partial y}\left(\mu\frac{\partial w}{\partial y}\right) \qquad (2)$$

This equation is differentiated with respect to s to obtain the necessary expression for $\partial w/\partial s$ in the plane of symmetry. The governing equations are completed with the equation of state, $p = \rho RT$ and Sutherland's viscosity law.

The initial data required to start the calculations are combinations of inviscid data obtained from the Jones tables[3] and boundary conditions at the wall including zero velocities and wall temperature. The Rankine-Hugoniot equations are used at the shock. There are two quantities which cannot be obtained directly. These are the second derivative of p and the first derivative of w in the crossflow direction. For the cases studied here, they are obtained from the Jones tables.[3]

The x-momentum, s-momentum, and energy equations can be linearized and then put into the standard parabolic equation form. To solve these equations, the first and second partial derivatives in the y-direction are replaced by a truncated Taylor series which allows for variable mesh spacing. The resulting finite-difference equations are of the tridiagonal form and are solved with the Thomas algorithm.[4] The continuity equation which is not parabolic in form is numerically integrated to obtain both the local shock standoff distance and normal velocity. The wall heat transfer (Q) is calculated using the product of the temperature gradient and the thermal heat conduction coefficient.

Results and Conclusions

The effects on the numerical solution of varying the mesh point grid and the shape of the starting profiles was investigated. It was found that the calculated flowfields are relatively insensitive to starting conditions and numerical grid mesh size.

To check the accuracy at zero angle of attack, solutions are calculated and compared with Peterson's[5] experimental results for helium flowing at $M_\infty = 16.4$ over a 10° half-angle cone. Agreement with the experimentally determined points is excellent

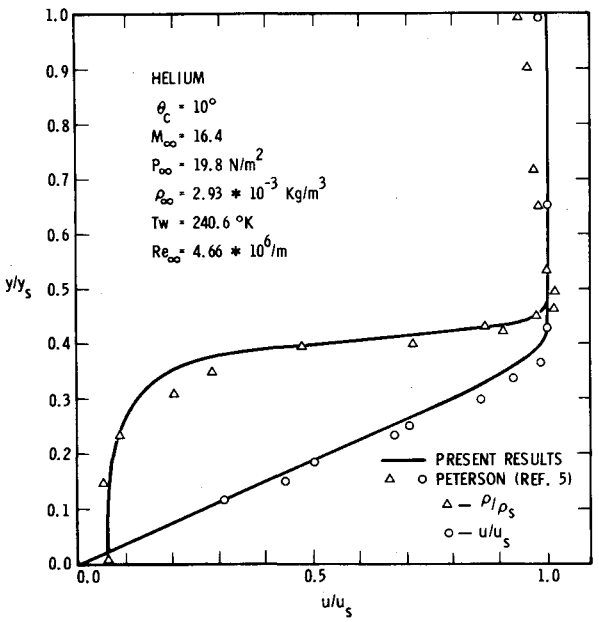

Fig. 1 Comparison of present results with those of Peterson.[5]

in the boundary layer, Fig. 1. The only region of any significant discrepancy is found in the density profile outside the boundary layer. The experimental data shows a density increase between the shock and the boundary-layer edge, while the code gives a zero density gradient. The increase corresponds with that predicted by the Jones tables.[3] The difference is attributed to the fact that the pressure in the code is taken to be constant between the shock and body for a given downstream value of x. Even with the discrepancy in density, the accuracy of the results is reasonable.

The program was also checked at nonzero angle. Shock shapes, streamlines, and heat-transfer data were investigated. Figure 2 shows how the shock standoff distances are affected by angle of attack, and compares these results with inviscid solutions.

Heat-transfer calculations have been made for a 15° half-angle cone at $M_\infty = 10.6$ and for angles of attack of 0°, 5°, and 10°. Freestream unit Reynolds number for this case is 1.3×10^6/m. These are the conditions used by Cleary[6] in the NASA Ames 3.5-ft hypersonic wind tunnel. The heat fluxes are also calculated using a simplified model of Reshotko.[7] A third method, the

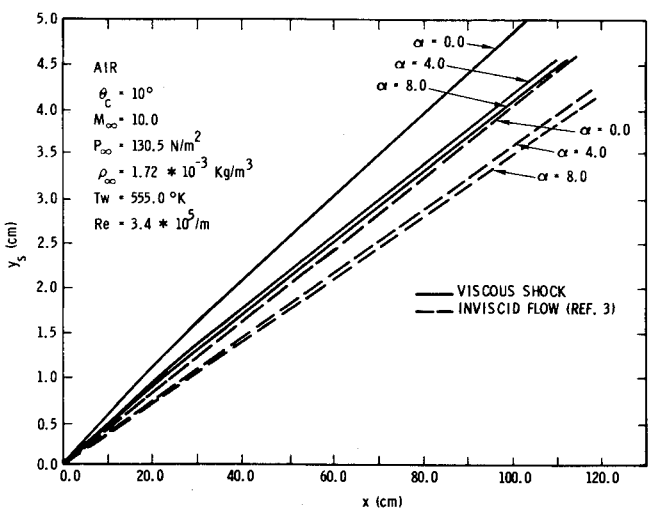

Fig. 2 Bow shock shapes compared with inviscid calculations.

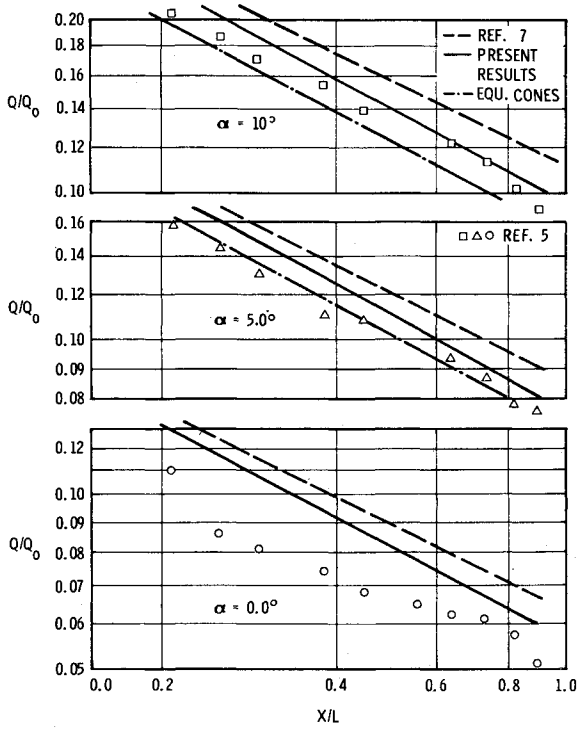

Fig. 3 Local heat transfer on a 15° cone, $Q_0 = 127.1$ kw/m^2.

method of equivalent cones, is used. Twenty and twenty-five degree cones are used to simulate the 5° and 10° angle of attack cases, respectively. Figure 3 shows the results of these calculations. All three theories and experimental data predict the same general trends; however, the experimental data lies lower than all theories.

The experimental results show 50% and 95% increases in heat-transfer rates at angles of attack of 5° and 10°, respectively. The equivalent cone method results in only half that gain. The present method and the Reshotko model give results which predict 40% and 75% increases in heat-transfer rates for angles of attack of 5° and 10°. These trends follow more closely the experimental prediction. In addition, the present calculation gives absolute values of heat transfer which are in better agreement with the experimental results than the Reshotko method.

In summary, the viscous shock layer technique developed here for three-dimensional flow in the windward plane of sharp cones at angle of attack gives results which agree well with other theories and experimental data. The method is easy to use and requires a minimum amount of computer time.

References

[1] Davis, R. T., "Numerical Solution of the Hypersonic Viscous Shock-Layer Equations," *AIAA Journal*, Vol. 8, No. 5, May 1970, pp. 843–851.

[2] Eaton, R. R. and Kaestner, P. C., "Viscous Shock Layer Flow in the Windward Plane of Cones at Angle of Attack," SC-RR-72 0449, Jan. 1973, Sandia Labs., Albuquerque, N. Mex.

[3] Jones, D. J., "Tables of Inviscid Supersonic Flow About Circular Cones at Incidence," AGARDograph 137, Nov. 1969.

[4] Richtmyer, R. D., *Difference Methods for Initial-Value Problems*, Interscience, New York, 1957, Chap. 9.

[5] Peterson, C. W., "An Experimental Study of Laminar Hypersonic Blunt Cone Wakes," *Astronautica Acta*, Vol. 15, 1969, pp. 67–76.

[6] Cleary, J. W., "Effects of Angle of Attack and Bluntness on Laminar Heating-Rate Distributions of a 15° Cone at Mach Number of 10.6," TN D-5450, Oct. 1969, NASA.

[7] Reshotko, E., "Laminar Boundary Layer with Heat Transfer on a Cone at Angle of Attack in a Supersonic Stream," TN 4152, Dec. 1957, NACA.

Flexibility Coefficients for Bending of a Disk under Sinusoidal Edge Loading

JOSEPH A. DOPKIN*
Ingersoll-Rand Company, Phillipsburg, N.J.
AND
TERRY E. SHOUP†
Rutgers University, New Brunswick, N.J.

Introduction

PREVIOUSLY published solutions for a disk under sinusoidal edge loading[1] have been specialized cases with a rigid block fixed to the inner radius, and the outer radius either fixed or simply supported. This paper presents a derivation and numerical tabulation of a set of flexibility coefficients which can be used to accommodate any boundary conditions which are compatible with first-order sinusoidal loading.

Analysis

The basic equations for a disk with arbitrary loading perpendicular to its surface are presented by Timoshenko and Woinowsky-Krieger.[2] For the special case of cosinusoidal edge loading only, the deflection can be written as

$$z = (Ar + Br^3 + Cr^{-1} + Dr \ln r) * \cos\alpha \tag{1}$$

where A, B, C, and D are constants to be determined for the particular problem.

This can be shown to satisfy the fundamental plate equation

$$\nabla^2 z = \left[\frac{\partial}{\partial r^2} + \frac{1}{r}\frac{\partial}{\partial r} + \frac{1}{r^2}\frac{\partial^2}{\partial \alpha^2}\right]\left[\frac{\partial z}{\partial r^2} + \frac{1}{r}\frac{\partial z}{\partial r} + \frac{1}{r^2}\frac{\partial^2 z}{\partial \alpha^2}\right] = 0 \tag{2}$$

It is convenient to further specialize the solution for the case of zero deflection at the inner radius, thereby using the plane of the inner radius as a coordinate plane as shown in Fig. 1.

For $z = 0$ at $r = b$, the constant A can be eliminated from Eq. (1), giving

$$z = r[(r^2 - b^2)B + (r^{-2} - b^{-2})C + D \ln \rho] \cos\alpha \tag{3}$$

and

$$\phi = \partial z/\partial r = [(3r^2 - b^2)B - (r^{-2} + b^{-2})C + D(\ln \rho + 1)] \cos\alpha \tag{4}$$

where $\rho = a/b$.

From Ref. 2

$$m = -\beta\{\partial^2 z/\partial r^2 + U[(1/r)\,\partial z/\partial r + (1/r^2)\,\partial^2 z/\partial \alpha^2]\}$$

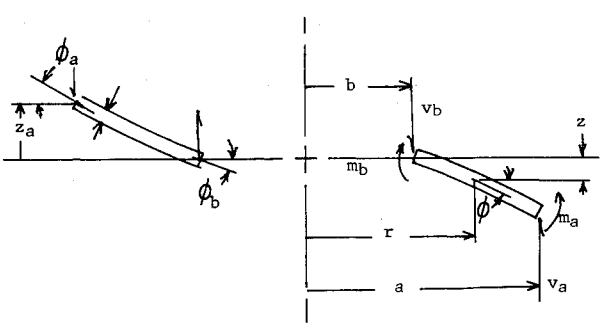

Fig. 1 Plate element in one-nodal diameter bending.

Received February 7, 1973; revision received April 18, 1973.
Index categories: Aircraft Vibration; VTOL Vibration; Structural Dynamic Analysis.

* Supervisor of Stress Analysis, Turbo Products Division.
† Assistant Professor, Mechanical and Aerospace Engineering Department.